polymer papers

Solution-grown crystals of isotactic polystyrene: neutron scattering investigation of the variation of chain trajectory with crystallization temperature

J. M. Guenet*
Institut Charles Sadron, (CRM-EAHP), CNRS-ULP, 6 rue Boussingault, 67083 Strasbourg Cedex, France

the late D. M. Sadler
H.H. Wills Physics Laboratory, Royal Fort, Tyndall Avenue, Bristol BS8 1TL, UK

and S. J. Spells
Department of Applied Physics, Sheffield City Polytechnic, Pond Street, Sheffield S1 1WB, UK
(Received 16 February 1989; revised 17 May 1989; accepted 23 May 1989)

Previous neutron scattering investigations carried out on isotactic polystyrene single crystals grown at 130°C from dilute solutions have revealed a sheet-like conformation and hence very regular chain folding. Here we report the same type of experiments performed on samples crystallized at $T_c = 75$, 85, 105 and 115°C. From the results in both the Guinier and the intermediate ranges, we come to the following conclusions: (i) At 115°C, we reproduce the results obtained at 130°C (regular folding in a single sheet). (ii) Decreasing T_c leads to a change of conformation for relatively high molecular weights (7×10^5 and 5×10^5). While crystallization still occurs along an $hk0$ plane, the regular folding is interrupted, leading both to superfolding and to crystallization in at least two different lamellae. (iii) For lower molecular weights (3×10^5 and 1.5×10^5) significant deviations from the sheet-like model appear only at $T_c = 85$°C. We conclude that above a critical molecular weight, which is temperature-dependent, irregularities in the folding habit take place. In this respect, polystyrene resembles polyethylene.

(Keywords: polystyrene; neutron scattering; chain folding; crystallization temperature)

INTRODUCTION

Knowledge of the chain trajectory in semicrystallized polymers has been and still is a major topic. Since the recent use and extension of neutron scattering as a powerful technique to probe molecular conformation, many papers have been devoted to the subject[1]. In this paper, we shall not consider all the situations of polymer crystallization but rather focus our attention on solution-grown crystals. Previous experiments reported by Guenet[2] on isotactic polystyrene (iPS) crystals grown at 130°C (that is at comparatively low undercooling) revealed that the chain trajectory resembles a thin sheet. This entails chain folding along an $hk0$ plane direction (seemingly 1 1 0) with adjacent or near-adjacent re-entry[3]. Alternatively, studies performed on polyethylene (PE) crystals, prepared at high undercooling so as to minimize isotopic segregation[4], have shown a more complex structure. According to Spells and Sadler[5], two phenomena occur simultaneously: (i) the chain folds back on an adjacent plane (superfolding) and (ii) although the proportion of adjacent re-entry is high (0.75), there is dilution along the fold plane with (an)other molecule(s). As stressed by these authors[5], these effects certainly arise from the competition that takes place between different chains while depositing onto the crystallization growth plane.

The polymer most extensively studied by neutron scattering, namely polyethylene, suffers from the problem of isotopic fractionation, due to the difference (of ~4°C) in the melting temperatures for the two isotopic species.

The phenomenon has been studied[6] by comparing the small-angle scattered intensity extrapolated to zero angle with the molecular weight measured independently (e.g. by g.p.c.). Debate continues on the nature of the isotopic inhomogeneity but, from a practical point of view, measurements on polyethylene are restricted to conditions of rapid crystallization. The zero-angle extrapolation can then be used as a check that fractionation is minimal. By contrast, in isotactic polystyrene there is negligible difference in the melting points, so that isotopic fractionation is virtually absent. A study of the chain trajectory at different crystallization temperatures is therefore possible. Such an investigation is much-needed so as to bridge the gap between these two polymers and therefore to discover whether iPS behaves like PE at larger undercoolings. The purpose of this paper is to report such experiments.

EXPERIMENTAL

Materials

Protonated and deuterated species were synthesized

* Present address and to whom correspondence should be addressed: Laboratoire de Spectrométrie et d'Imagerie Ultrasonores, Unité Associée au CNRS, Université Louis Pasteur, 4 rue Blaise Pascal, F-67070 Strasbourg Cedex, France

0032-3861/90/020195-07$03.00

Table 1 Molecular-weight characteristics of the deuterated samples

M_w	M_w/M_n
1.54×10^5	1.13
3×10^5	1.2
5×10^5	1.2
7×10^5	1.32

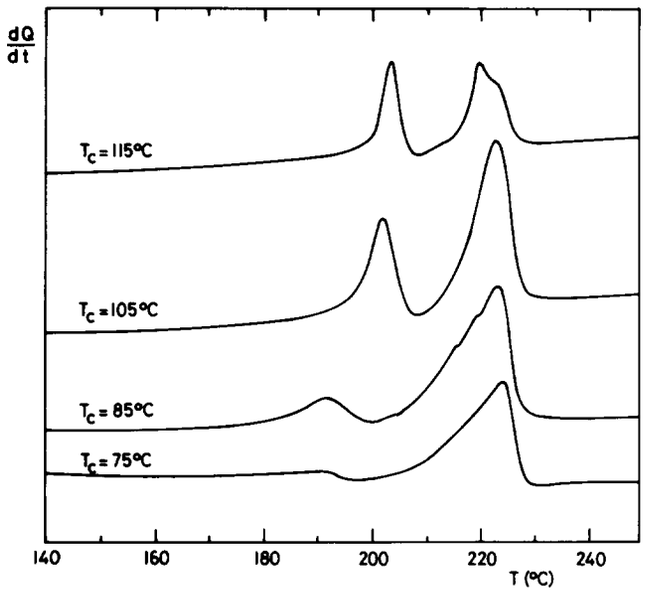

Figure 1 D.s.c thermograms (heating rate 10°C min^{-1}) for the various crystallization temperatures

following the well known Natta method[7]. Once prepared, the polymer was treated in boiling heptane for 12 h and then in methyl ethyl ketone (MEK) at room temperature so as to remove the atactic content[8]. The deuterated samples were fractionated with toluene–ethanol at 50°C[9]. All the samples possess a stereoregularity better than 98% as ascertained by ^{13}C n.m.r. investigations. Molecular weights and molecular-weight distributions were obtained from g.p.c. in tetrahydrofuran (THF)[9]. Sample characteristics are listed in *Table 1*. The hydrogenated polymer is characterized by $M_w = 3.2 \times 10^5$ and $M_w/M_n = 2.8$.

Sample preparation

Clear solutions of 0.66% w/v of iPS, of which ~1% w/w are deuterated chains, were prepared in dibutyl phthalate by heating at 190°C. Crystal growth was achieved by quenching these solutions into oil baths held within ±0.1°C at the desired crystallization temperature (namely, 75, 85, 105 and 115°C). The self-seeding technique was avoided in order to make sure that all the samples were crystallized under exactly the same conditions. Although 4–7 days of crystallization were needed to obtain a reasonable yield (25% conversion), no noticeable degradation was detected. The crystalline material was then recovered by filtration, washed with toluene and dried out under vacuum at room temperature. Disc-shaped samples of 1 mm thickness and 12 mm diameter were prepared by compression-moulding under vacuum at 140°C.

Characterization

Differential scanning calorimetry (d.s.c.). A Perkin–Elmer DSC II device equipped with the TADS system has been used to characterize the thermal behaviour of the crystals. Approximately 5 mg of material were placed into a d.s.c. pan. A heating rate of 10°C min^{-1} was used and the apparatus was calibrated with indium. The value[10] of $\Delta H = 2000$ cal mol^{-1} was taken to determine the percentage crystallinity x_c. D.s.c. thermograms are given in *Figure 1* and values of x_c in *Table 2*.

Electron microscopy. A Hitachi HU 11CS microscope was used. Samples were shadowed with Pt/C and carbon-coated in the usual manner. Results are listed in *Table 2*.

These figures for lamellar thickness are somewhat smaller than typical values of around 6–7 nm for the long period, as measured by small-angle X-ray diffraction on samples crystallized in similar solvents[11]. The range of crystallization temperature used here is, however, expected to lead to little variation in lamellar thickness.

Neutron scattering

All the experiments were performed at the Institut Laue–Langevin (ILL), Grenoble, with D11 and D17 small-angle cameras. The available range of momentum transfer $q = (4\pi/\lambda)\sin(\theta/2)$ ranged from 5×10^{-3} to 1.5×10^{-2} Å^{-1} for D11 and from 10^{-2} to 10^{-1} Å^{-1} for D17.

On both apparatuses, a mechanical wavelength selector was used, which provides a spectrum characterized by a relative width at half-height of $\Delta\lambda/\lambda = 10\%$. All the experiments were normalized with water and corrected for transmission and thickness. The excess intensity scattered by the labelled chains was obtained after subtracting the signal of a blank sample containing protonated chains only, crystallized under the same conditions.

THEORETICAL

Two types of information can be gained from neutron scattering depending on the range of momentum transfer q.

(i) The *Guinier* range:

$$I(q) \simeq M_w(1 - q^2R_g^2/3)$$

The intensity $I(q)$ is directly proportional to the weight-average molecular weight M_w of the labelled species. In addition, the variation of $I(q)$ with q^2 is linear, with a slope proportional to the mean-square radius of gyration of the labelled chains.

(ii) The *intermediate* range—usually, $I(q)$ reduces to:

$$I(q) \simeq q^{-\alpha}$$

where α is dependent on the chain conformation.

The calculation of neutron scattering intensities from molecular models can be carried out in several ways. One possibility involves structures of specific geometry and

Table 2 Degree of crystallinity from d.s.c. and lamellar thickness from electron microscopy as a function of crystallization temperature

T_c (°C)	x_c (%)	l_c (Å)
115	63	50±5
105	44	49±5
85	41	45±5
75	39	

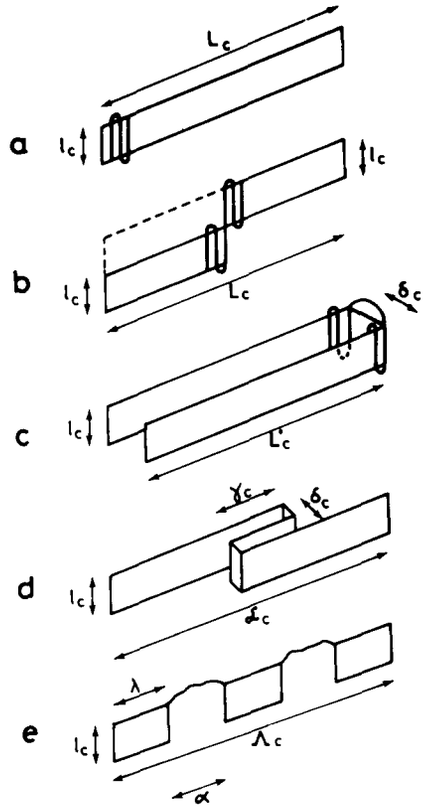

Figure 2 Possible models for chain crystallization in solution-grown crystals: (a) sheet-like model, (b) hinge-like model, (c) superfolded model, (d) Z-like model, (e) dilution model

with specific dimensions. Within these structures, the chain folding is assumed to be regular. This approach has previously been used for iPS crystals[2,12]. Another possibility would be to take a specific structure and allow the statistics of chain folding to be varied within that structure. This method has been employed in the case of polyethylene single crystals[5]. In the present work, we recognize that chain folding in iPS tends to produce sheet-like structures, but we wish to consider different ways of combining these sheets. We therefore adopt the first approach outlined above. No attempt will be made to calculate the entire intensity pattern as a function of q, but instead we will determine the various types of behaviour in both the Guinier and intermediate ranges defined above.

For the sake of brevity and clarity, we will restrict our attention to five schematic models (*Figure 2*), each possessing a specific characteristic. Obviously, the actual chain trajectory may be a combination of these models. Another parameter, which is not taken into account here, would be the regularity of folding within any structure.

The sheet-like model (Figure 2a)

This model is well suited to describe the case where the chain folds regularly in one lamella either within a single $(hk0)$ plane or alternately within two sets of planes, in the latter case producing a 'zigzag' incorporation of crystal stems[3].

As long as the value of q is such that $qI \ll 1$ and $q\varepsilon \gg 1$ (I is the re-entry length[12] and ε the chain cross-section), the form factor $P(q)$ derived by Porod[13] for this model can be used:

$$P(q)=\frac{2}{qL_c}\left[\frac{\pi'}{ql_c}\left(\int_0^{ql_c}\frac{J_1(x)}{x}\,dx\right)+\frac{1}{qL_c}\left(\frac{\sin(ql_c/2)}{ql_c/2}\right)^2-\frac{\sin(qL_c)}{(qL_c)^2}\right] \quad (1)$$

where L_c and l_c are respectively the length and the width of the sheet (l_c therefore being close to the value of the lamellar thickness) and π' is a complex function that rapidly reaches the value $\pi = 3.14\ldots$ beyond the Guinier regime. Such a form factor is theoretically only valid for $L_c \gg l_c$.

The radius of gyration of such a conformation reads:

$$R_g^2=\frac{L_c^2}{12}+\frac{l_c^2}{12} \quad (2)$$

A somewhat more elaborate relationship can be derived which takes into account the amorphous loops[12]. However, this mainly affects the magnitude of R_g^2 but not its behaviour with molecular weight. In principle, the variation of R_g^2 with molecular weight should display two regimes. For a molecular weight such that $l_c \gg L_c$, $R_g^2 = l_c^2/12$, whereas for $l_c \ll L_c$, $R_g^2 = L_c^2/12$. In the first case, R_g^2 varies little with molecular weight while in the second case $\langle R_g^2\rangle^{1/2}$ is directly proportional to the labelled chain molecular weight. The second case has been experimentally observed for isotactic polystyrene[2].

Interestingly enough, two types of asymptotic behaviour are expected for $P(q)$ in the intermediate range.

For $ql_c \ll 1$ and $qL_c > 1$:

$$I(q)\simeq M_w\left[\frac{\pi}{qL_c}\exp\left(-\frac{q^2l_c^2}{24}\right)\right] \quad (3)$$

The exponential term is only a slight correction so that a q^{-1} behaviour should be observed (especially if $L_c \gg l_c$). From a plot of $\log qI(q)$ vs. q^2, l_c^2 can be determined as well.[2]

For $ql_c > 1$ and $qL_c > 1$:

$$I(q)\simeq M_w\left(\frac{2\pi}{q^2l_cL_c}\right) \quad (4)$$

These two types of behaviour can be easily evidenced by means of a Kratky plot, $q^2I(q)$ vs. q (see *Figure 3*).

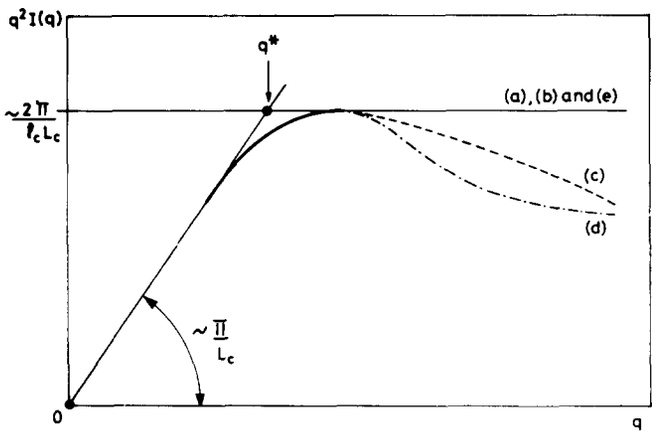

Figure 3 Theoretical variation of the scattered intensity, plotted with a Kratky plot, $q^2I(q)$ vs. q: (a), (b) and (e) correspond to the sheet-like, the hinge-like or the dilution models (the value of the ordinate $2\pi/l_cL_c$ is only valid for the sheet-like model), (c) to the superfolded model and (d) to the Z-like model

Two linear asymptotes are obtained for each regime. The first one has a slope proportional to πL_c^{-1} and must extrapolate to $I(q)=0$ for $q=0$. The second one is constant with q with an ordinate proportional to $2\pi(l_c L_c)^{-1}$. These two linear asymptotes intercept at q^* given by:

$$q^* = 2/l_c \tag{5}$$

Thus, the value of l_c can be obtained in two ways from SANS data (from relation (3) with a plot of $\log qI(q)$ vs. q^2 and from relation (5)) and compared to that determined by other techniques. If the values are close and the different types of behaviour described above are found, one may safely conclude that the chain folds regularly along the crystal growth plane.

It is worth mentioning that a q^{-2} behaviour is also observable for a Gaussian chain whereas a q^{-1} behaviour is not.

The hinge-like model (Figure 2b)

True single crystals are difficult to prepare and, at high undercoolings especially, clusters of lamellae are usually obtained. One may then wonder whether the chain does not crystallize in more than one lamella. Here, we consider the schematic situation where half the chain crystallizes in one lamella and then the other half completes crystallization into an upper (or lower) lamella. Two cases are to be envisaged: either the chain keeps on crystallizing in the same direction (forward) or it reverses its direction (backward) in the second lamella. There is no physical argument to favour either case. Accordingly, we shall consider the probability of each process to be 0.5. This model is different from the CAC model defined in a previous publication[12], in that there is no significant amorphous portion between the two sheets.

Provided that the inequality $l_c < L_c/2$ is still valid (which should hold as long as iPS is concerned), we deduce:

$$R_g^2 = \frac{5l_c^2}{24} + \frac{5L_c^2}{96} \tag{6}$$

While the law $R_g \simeq M^\nu$ with $\nu \simeq 1$ may still be observed, the value of R_g should be affected when compared to regular folding in one lamella (approximately 40%).

Trivial calculations making use of the developed form of the exponential term further show for $I(q)$ in the intermediate range:

$$I(q) \simeq \frac{3\pi}{2qL_c} \exp\left(-\frac{q^2 l_c^2}{28}\right) \tag{7}$$

$$I(q) \simeq \frac{2\pi}{q^2 l_c L_c} \tag{8}$$

The slope of the q^{-1} behaviour should then be affected by a factor 1.5. If comparison is possible with a regularly folded chain in one lamella, the difference is observable experimentally.

In addition q^* reads:

$$q^* = 4/(3l_c) \tag{9}$$

This implies that if l_c is calculated according to $l_c = 2/q^*$ one should end up with a discrepancy of about 50% when compared to the value found by electron microscopy (EM) or X-ray techniques.

However, it is worth keeping in mind that, in reality, hinge-like models are certainly not symmetric. Should there be only a slight asymmetry, the above calculations are good approximations. Conversely, if the asymmetry goes as far as to have only a small part crystallizing in another lamella, there is no chance to detect it since the behaviour would not be significantly different from that of a chain regularly folded in one lamella.

The superfolding model (Figure 2c)

This model proposed by Sadler and Keller[4] has been found to account for the SANS results gained on polyethylene crystallized at high undercoolings. In that model R_g^2 reads:

$$R_g^2 = \frac{l_c^2}{12} + \frac{L_c'^2}{12} \tag{10}$$

with $L_c' = L_c/(n+1)$, n being the number of superfolds. For a large number of superfolds, $L_c^2 \simeq l_c$ in which case R_g can be almost invariant with molecular weight as already experimentally observed for PE ($R_g \simeq M^{0.1}$)[4].

For n superfolds, provided $l_c \gg n\delta_c$, $I(q)$ reads in the intermediate range:

$$I(q) \simeq \frac{\pi}{qL_c'} \exp\left(-\frac{q^2 l_c^2}{24}\right) \quad \text{for } ql_c < 1 \text{ and } qL_c > 1 \tag{11}$$

$$I(q) \simeq \frac{2\pi}{q^2 l_c L_c'} \exp\left(-\frac{q^2 n^2 \delta_c^2}{24}\right) \quad \text{for } ql_c > 1 \text{ and } qL_c' > 1 \tag{12}$$

In relation (12), a corrective term takes into account the fact that one is no longer dealing with a thin sheet but a 'thick' one. Owing to this additional term, a decrease of the term $q^2 I(q)$ is expected: hence the shortening or the absence of the plateau in the Kratky plot (see *Figure 3e*). Besides, if δ_c comes close to l_c, the conformation cannot be treated any longer as a small perturbation of the thin sheet. We have now to consider a two-scattering-density system for which $I(q)$ reads:

$$I(q) \simeq q^{-4} \times S/V \tag{13}$$

where S is the surface area and V the volume of the object.

Alternatively, if L_c' is larger than l_c, the q^{-1} behaviour should still exist, otherwise it will also vanish, resulting in the observation of only the q^{-4} decay.

The Z-like model (Figure 2d)

Now R_g^2 reads, provided $\delta_c < l_c$:

$$R_c^2 = \frac{l_c^2}{12} + \frac{\mathscr{L}_c^2}{12} = \frac{l_c^2}{12} + \frac{\sigma L_c^2}{12} \tag{14}$$

$\mathscr{L}_c$ is the actual length, L_c is the contour length (the length once the Z is unfurled) and σ is a function of both γ_c and δ_c. In such a model, γ_c and δ_c may be molecular-weight-dependent, which entails a non-trivial variation of R_g with this latter parameter.

If $\delta_c < l_c$ and $l_c < \mathscr{L}_c$, $I(q)$ exhibits the following types of behaviour:

$$I(q) \simeq \frac{\pi}{q\mathscr{L}_c} \exp\left(-\frac{q^2 l_c^2}{24}\right) \tag{15}$$

$$I(q) \simeq \frac{2\pi}{q^2 l_c \mathscr{L}_c} \exp(-k'\delta_c^2) \tag{16}$$

If $\delta_c \simeq l_c$, first the q^{-1} behaviour may vanish. Secondly,

at larger q, $I(q)$ should read:

$$I(q) \simeq \frac{2\pi}{q^2 l_c \mathscr{L}_c} + \frac{K(\gamma_c, \delta_c)}{q^4} \quad (17)$$

where K is a constant depending on parameters γ_c and δ_c. Such a conformation will lead to a broad maximum followed by an asymptotic behaviour reaching q^2 in the Kratky representation (this is so since $q^{-2} > q^{-4}$ at larger q) (*Figure 3d*).

The dilution model (*Figure 2e*)

Regular folding interrupted by non-adjacent folds may be represented by this model. This corresponds to a dilution of the labelled molecule along the growth face of (an)other molecule(s), as has been proposed to be a general feature in polyethylene crystals[5]. For polyethylene, a statistical distribution of crystal stems was used, leading to a distribution in lengths λ and α.

The case with fixed values of λ and α seems unrealistic and is accordingly not treated here. However, if such were the case, a peak should be visible at $q = 2\pi/(\lambda+\alpha)$, arising from the periodicity.

The effect of sheet interruption can be taken into account by assuming in a first approximation that only the scattering power per unit area is altered. This results in:

$$I(q) \simeq \frac{\pi}{q\Lambda_c} \frac{\lambda}{\lambda+\alpha} \exp\left(-\frac{q^2 l_c^2}{24}\right) \quad (18)$$

$$I(q) \simeq \frac{2\pi}{q^2 p l_c (\lambda+\alpha)} \quad (19)$$

where p is the number of $\lambda+\alpha$ subunits. This entails for q^*:

$$q^* = \frac{2\Lambda_c}{\lambda p l_c} \quad (20)$$

As $\lambda p/\Lambda_c < 1$, the apparent thickness $l_{c,app} = 2/q^*$ should be lower than the actual one. As to R_g, it is larger than that of regular folding and reads:

$$R_g^2 = \frac{l_c^2}{12} + \frac{p^2(\lambda+\alpha)^2}{12} \quad (21)$$

In this section, we have so far not considered which fold plane(s) is (are) involved. A zigzag folding model with stems in adjacent sites has been proposed on the basis of wide-angle neutron scattering measurements[3]. An alternative model, with folding within a single plane, would involve next-to-adjacent folding. In principle, we should be able to distinguish between these folding habits in the case of models (a) and (b) (*Figure 2*) through the dimension L_c, which is related to R_g (equations (2) and (6)). Conversely in order to fit experimental radius-of-gyration data to any of models (c), (d) or (e) requires an arbitrary choice of model dimensions (e.g. L_c' and δ_c in case (c)). The different folding models would give rise to different pairs of values for L_c' and δ_c in this case, and neither quantity can be determined independently. For this reason, we do not consider here the type of folding habit.

RESULTS AND DISCUSSION

Unlike the samples crystallized at 130°C[2], for which it was shown that the chain trajectory is not molecular-weight-dependent (at least in the investigated range of molecular weights), samples crystallized at lower temperatures do exhibit a variation with this parameter. Hence, in the relation $R_g \simeq M^v$, v is no longer a constant, so that it is impossible from the Guinier range to favour one type of model. As a consequence, much of the interpretation given herein is derived from the data gained in the intermediate range. The values of R_g are then useful to discover whether there is any inconsistency.

A convenient way of presenting and discussing the results consists of separating the 'high' molecular weights (7×10^5 and 5×10^5) from the 'low' ones (3×10^5 and 1.5×10^5).

'High' molecular weights (7×10^5 *and* 5×10^5)

$T_c = 115°C$. At this crystallization temperature, the intensity scattered in the intermediate range displays all the characteristics of the form factor of a thin sheet (*Figure 4*). The q^{-1} behaviour as well as the q^{-2} behaviour are well evidenced. The value of l_c determined from q^* is slightly lower than that measured by EM. It is suspected that, unlike the samples crystallized at 130°C, there is more interruption of the folding regularity at this temperature.

However, it can be concluded that the chain trajectory at $T_c = 115°C$ is not that different from the one at $T_c = 130°C$. We note further that the degree of crystallinity is high ($x_c = 63\%$) and that the d.s.c. thermogram is characteristic of well organized crystals[14]. Therefore, if there is a relation between the crystal perfection and the chain trajectory, the above results are not surprising.

$T_c = 105°C$. Crystallization at this temperature leads to the occurrence of deviations from regular folding (*Figures 4* and *5*). While the q^{-1} behaviour is still observed, the pure q^{-2} behaviour is virtually absent and replaced by either a $q^{-\alpha}$ with $\alpha > 2$ or $q^{-2}\exp(-q^2n^2\delta_c^2/24)$. We conclude that superfolding has taken place.

Values of R_g (see *Table 3*) are just slightly lower than those measured for samples crystallized at 130°C (417 Å instead of 450 Å and 290 Å instead of 330 Å), suggesting that the decrease of R_g due to superfolding is compensated by the interruption of regular folding. Values of l_c (see *Table 4*) determined either by $2/q^*$ or from the slope

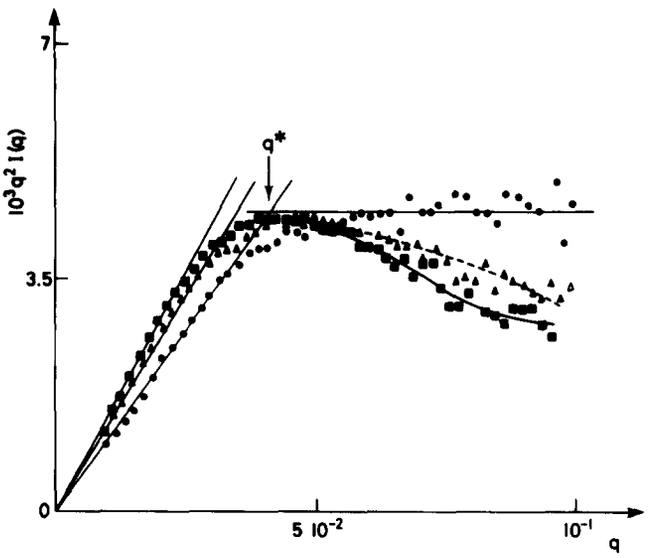

Figure 4 Kratky plot, $q^2I(q)$ vs. q, for $M_{w,iPSD} = 5\times10^5$: (●) T_c = 115°C, (▲) T_c = 105°C, (■) T_c = 85°C (arbitrary units)

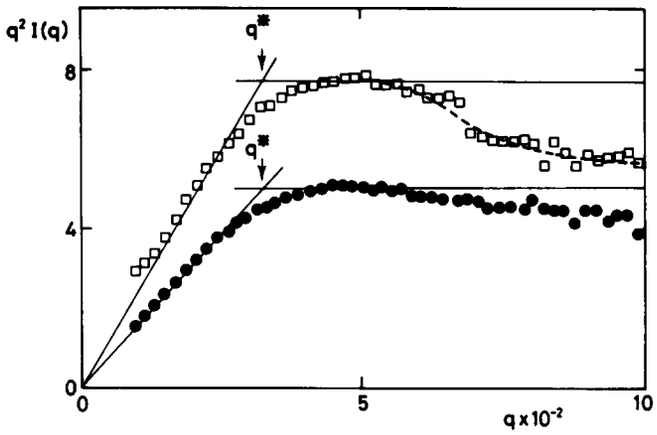

Figure 5 Kratky plot, $q^2I(q)$ vs. q, for $M_{w,iPSD}=7\times10^5$: (●) $T_c=105°C$, $T_c=85°C$ (arbitrary units)

Table 3 Values of the radius of gyration as a function of molecular weight and crystallization temperature

T_c (°C)	$M_{w,iPSD}$	R_g (Å)
130 (from ref. 2)	1.54×10^5	110±10
	5×10^5	330±30
	7×10^5	450±40
105	1.54×10^5	150±30
	5×10^5	290±30
	7×10^5	417±50
85	5×10^5	260±20
	7×10^5	326±40
75	7×10^5 ($M_{w,SANS}=1.8\times10^5$)	136±10

Table 4 Lamellar thicknesses at different temperatures as determined from: (a) electron microscopy; (b) $l_c=2/q^*$; (c) $\log qI(q)$ vs. q^2

		l_c (Å)		
M_w	T_c (°C)	(a)	(b)	(c)
7×10^5	105	49±5	59	66
	85	45±5	–	74
5×10^5	115	50±5	50	53
	105	49±5	59	58
	85	45±5	–	71
3×10^5	85	45±5	52	48
1.5×10^5	105	49±5	39	54
	85	45±5	44	41

in the $\log qI(q)$ vs. q^2 representation are in good agreement with those measured by EM. This fact is acceptable if one considers that the apparent decrease of l_c from $2/q^*$ due to sheet interruption is compensated by superfolding.

Accordingly, the chain trajectory can be schematically described here with a model encompassing the superfolded and the dilution models.

$T_c=85°C$. The general trend is to find enhanced deviation from the thin sheet structure (*Figures 4* and 5). The q^{-1} behaviour is still evidenced, yet not so unambiguously. Any q^{-2} dependence can be regarded as totally absent. Determination of l_c by $l_c=2/q^*$ obviously becomes irrelevant in such a case. The value of l_c for both label molecular weights determined from the plot of $\log qI(q)$ vs. q^2 is larger than the directly measured one. This suggests crystallization in more than one lamella. In addition, it would seem that the intensity tends towards a q^{-2} behaviour at larger angles. According to the theoretical analysis, this would imply the existence of a central core.

Concerning R_g (*Figures 6* and 7), there is a strong decrease of its value for $M_w=7\times10^5$ and a moderate one for $M_w=5\times10^5$ (see *Table 3*). (We note that the slope in the q^{-1} regime is consistent with such values.) The intermediate-range results are consistent with a model made up with a combination of hinge-like model and central core. Values of R_g suggest, as above, that interruption of regular folding still takes place. Eventually, it appears that at such crystallization temperatures virtually all types of deviations from the thin sheet envisaged in the theoretical section occur for molecular weights of 5×10^5 and above. There is evidently a link with the thermal properties: (i) the thermograms are characteristic of less organized crystals and (ii) the crystallinity has dropped down to $x_c=0.4$, which might be the result of large amounts of regular folding interruption.

$T_c=75°C$. Only one labelled molecular weight has been investigated ($M_{w,iPSD}=7\times10^5$). The results are puzzling: not only is $R_g=136$ Å a very low value for that

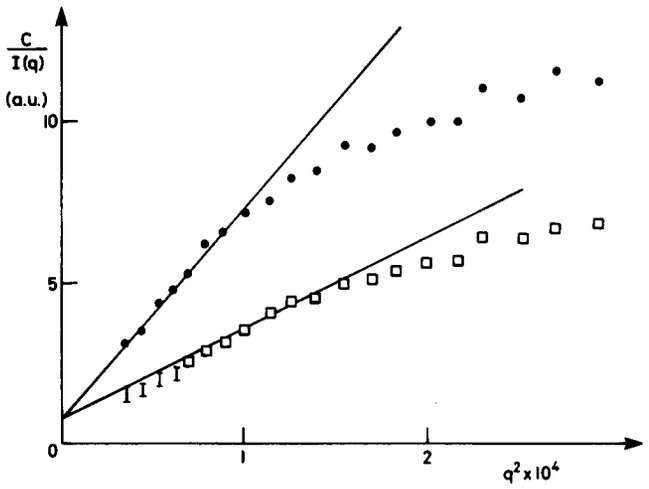

Figure 6 Zimm plot, C/I (q) vs. q^2, for $M_{w,iPSD}=7\times10^5$: (●) $T_c=105°C$, (□) $T_c=85°C$ (arbitrary units)

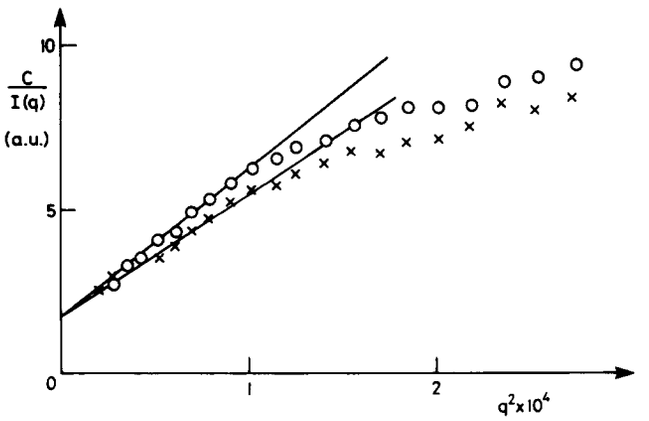

Figure 7 Zimm plot, $C/I(q)$ vs. q^2, for $M_w=5\times10^5$: (○) $T_c=105°C$, (×) $T_c=85°C$ (arbitrary units)

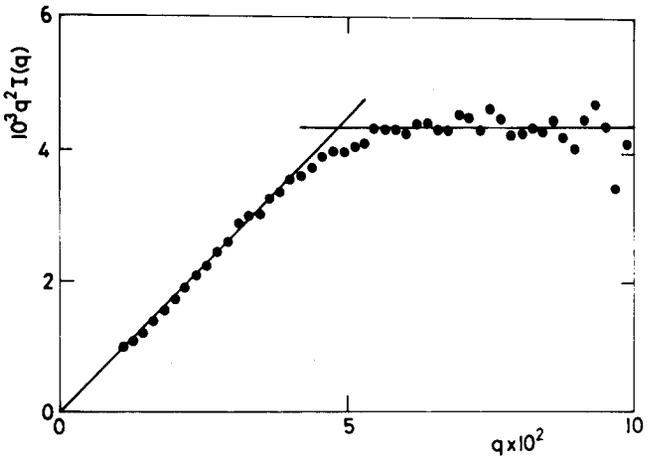

Figure 8 Kratky plot, $q^2I(q)$ vs. q, for $M_{w,iPSD}=1.54\times10^5$: (●) $T_c=105°C$ (arbitrary units)

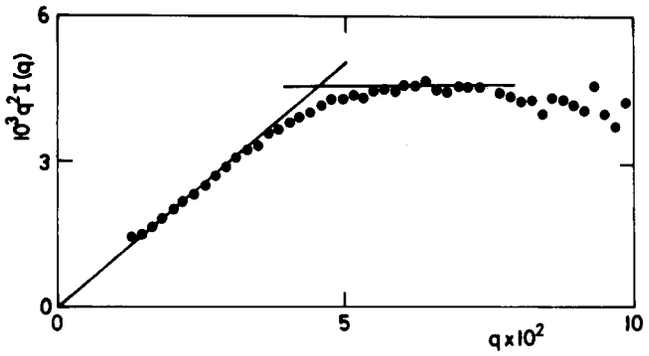

Figure 9 Kratky plot, $q^2I(q)$ vs. q, for $M_{w,iPSD}=1.54\times10^5$: (●) $T_c=85°C$ (arbitrary units)

deuterated sample (even in the Gaussian state[15]), but the molecular weight determined by neutrons is about four times smaller than the actual one. Clearly, further investigations are needed to allow one to propose a model. Yet these observations are consistent with a molecule folding in more than one lamella, the lamellae being separated by a distance that is large compared with $l_c/2$. In this case the experimental q range does not correspond to the Guinier range for the complete molecule, and a smaller 'effective' radius of gyration and molecular weight would be determined. Similar experimental behaviour has been observed in solution-crystallized polyethylene of high molecular weight[16].

'Lower' molecular weights (3×10^5 and 1.5×10^5)

$T_c=105°C$. For $M_{w,iPSD}=1.5\times10^5$, the intensity pattern recorded in the intermediate range resembles closely the one obtained for $M_w=5\times10^5$ at $T_c=115°C$ (*Figure 8*). Accordingly, this labelled low molecular weight adopts a thin sheet conformation.

As above (see *Table 4*), the low value of l_c determined by $2/q^*$ and correspondingly its discrepancy when compared to that determined by a Porod plot suggest that the sheet is not continuous but interrupted from place to place. The fact that R_g is also slightly larger than expected (150 Å instead of 110 Å) is consistent with the existence of sheet interruption.

$T_c=85°C$. At this crystallization temperature for $M_w=1.5\times10^5$ the conformation differs from the thin sheet very slightly (*Figure 9*). This suggests that some chains still possess a thin sheet conformation while others have

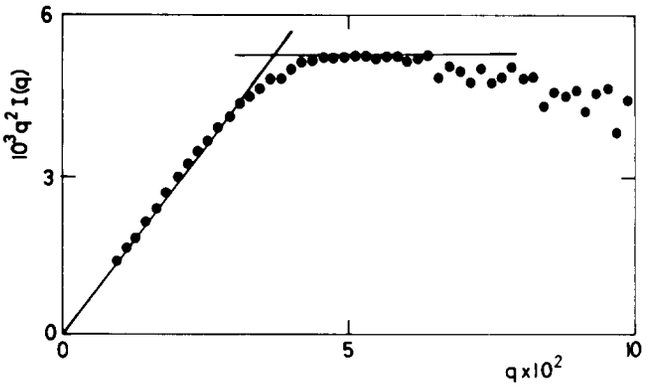

Figure 10 Kratky plot, $q^2I(q)$ vs. q, for $M_{w,iPSD}=3\times10^5$: (●) $T_c=85°C$ (arbitrary units)

'superfolded', the proportion of these latter certainly being small.

Conversely, for $M_w=3\times10^5$ the deviation is quite perceptible (*Figure 10*), yet not so enhanced as with $M_w=5\times10^5$. Curiously enough, l_c determined either by $q^*=2/l_c$ or a Porod plot are in agreement with that found by EM. It is suspected as previously that some compensation takes place due to the simultaneous occurrence of superfolding and folding interruption.

CONCLUSIONS

In this paper, we confirm previous findings by Guenet[2] showing that the chain trajectory at relatively low undercoolings is regularly folded, thus resembling a thin sheet. In addition, it is shown that lowering the crystallization temperature introduces irregularities in the folding habit for high molecular weights (7×10^5 and 5×10^5) while lower molecular weights are almost unaffected.

Accordingly, the chain trajectory in iPS solution-grown crystals is dependent on both the crystallization temperature and the molecular weight. These results show that iPS at low undercoolings behaves virtually as does polyethylene.

ACKNOWLEDGEMENT

We are indebted to the staff of the ILL, Grenoble, for experimental assistance.

REFERENCES

1 See for instance 'Organisation of Macromolecules in the Condensed Phase', Faraday Disc. Chem. Soc. 68, 1980
2 Guenet, J. M. *Macromolecules* 1980, **13**, 387
3 Sadler, D. M., Spells, S. J., Keller, A. and Guenet, J. M. *Polym. Commun.* 1984, **25**, 290
4 Sadler, D. M. and Keller, A. *Polymer* 1976, **17**, 37
5 Spells, S. J. and Sadler, D. M. *Polymer* 1984, **25**, 739
6 Schelten, J. and Ballard, D. G. H. *Polymer* 1974, **15**, 682
7 Natta, G. *J. Polym. Sci.* 1955, **16**, 143
8 Utiyama, H. *J. Phys. Chem.* 1965, **69**, 4138
9 Guenet, J. M., Gallot, Z., Picot, C. and Benoit, H. *J. Appl. Polym. Sci.* 1977, **21**, 2181
10 Dedeurwaerder, R. and Oth, J. F. M. *J. Chim. Phys.* 1959, **56**, 940
11 Overbergh, N., Girolamo, M. and Keller, A. *J. Polym. Sci., Polym. Phys. Edn.* 1977, **15**, 1475
12 Guenet, J. M. and Picot, C. *Polymer* 1979, **20**, 1473
13 Porod, G. *Kolloid Z.* 1951, **124**, 83
14 Wunderlich, B. 'Macromolecular Physics', Vol. II. Academic Press, New York, 1973
15 Guenet, J. M., Picot, C. and Benoit, H. *Macromolecules* 1979, **12**, 868
16 Spells, S. J. and Sadler, D. M. unpublished results